



## Modeling and dynamic analysis of a membrane bioreactor with backwash scheduling

Raafat Alnaizy\*, Nabil Abdel-Jabbar, Ahmed Aidan, Noor Abachi

*Department of Chemical Engineering, American University of Sharjah, PO Box 26666, Sharjah, United Arab Emirates*

*Tel. +971 6 515 2710; Fax: +971 6 515 2979; email: ralnaizy@aus.edu*

Received 17 July 2011; Accepted 15 January 2012

---

### ABSTRACT

A dynamic model, based on mass transport and reaction rate laws of biomass and substrate for a membrane bioreactor (MBR), was successfully developed. Furthermore, an empirical model for flux prediction was used. Key kinetic model parameters were estimated via non-linear fitting of the model predictions to experimental data obtained from current and previous works. The performance of the MBR was evaluated with different vacuum-to-backwash time ratio. Permeate flux dynamics were shown to be sensitive to the backwash scheduling scenario. The proposed model will enable optimization of MBR operation in an attempt to minimize membrane fouling.

*Keywords:* MBR; Biomass; Sludge; Dynamic; TMP; Fouling

---

### 1. Introduction

One of the main challenges in membrane bioreactor (MBR) operation is membrane fouling [1,2]. The fouling layer blocks the membrane pores, decreases permeate flux, increases pressure drop across the membrane, reduces permeate production, and biodegrades the membrane. The severity of fouling is determined by a combination of various physical, chemical, and biological operating factors [3]. Also it is the phenomena responsible for increasing the membrane hydraulic resistance which is referred to as permeate flux or permeability through the membrane pores [4]. Many attempts were made to minimize and control fouling such as backwash and aeration [5–8]. Backwash is effective in removing fouling due to pore blocking and removing the loosely attached accumulated foulants on the membrane surface (cake layer). Other methods to

clean and regenerate the membrane include intermittent filtration, chemical cleaning, and air cleaning.

Optimization of frequency and duration of backwash scheduling is essential to reduce energy and permeate consumption and to control membrane fouling. The importance of this optimization arises from the fact that very frequent backwashing may damage the pump and membrane, also it may affect the net volume of permeate. Conversely, less frequent backwashing leads to severe membrane fouling. Many researchers (Yigit et al. [5], Jiang et al. [8], and Aidan et al. [9]) investigated the significant association between backwash time and filtration time for an MBR system. They evaluated different scenarios and investigated their effects on the permeate flux. All three studies revealed that longer backwash time was an effective method for fouling control. Simultaneously, they agreed that less frequent backwash was more efficient because of the role of accumulation in the cake layer. The cake layer acts as a pre-filter preventing direct contact of fine particles (colloidal and solutes) with the membrane and

---

\*Corresponding author.

reduces membrane pore blocking (irreversible fouling). Results revealed an increase in both vacuum and backwash pressures as flux decreases. The increase in vacuum indicates a decrease in pressure across the membrane during filtration, causing the decline in flux and the presence of membrane fouling. Conversely, the increase in backwash pressure throughout the backwash period also indicates the increase in the severity of fouling and possibly the occurrence of irreversible fouling. Therefore, a higher backwash pressure will be required to clean the membrane. It was concluded that less fluctuation in backwash pressure through operation indicated optimum backwash scheduling ratio. The reported optimum was to conduct less frequent but longer backwash period with vacuum-to-backwash ratio of 10 min vacuum to 2 min backwash [9].

Based on the above observations, there is a need to study dynamic behavior of MBR with different operating scenarios in order to optimize its performance. However, this task can be very expensive and laborious since it needs trial experimentation on the actual process. Therefore, it is imperative to develop a detailed physical model that mimics the process. The model simulation numerical results will then be used in prediction of the process behavior under different conditions, which can be utilized in optimization and control of MBR.

Several modeling approaches were proposed to model membrane performance. Redkar and Davis [10] have obtained excellent experimental results for various combinations of transmembrane pressures, back-pulsing, and forward filtration times. Although the theory they have developed is qualitatively useful, quantitative predictions are far from acceptable as pointed by Mallubhotla and Belfort [11], who proposed a semi empirical model of cross-flow filtration with periodic back-pulsing. Tien and Bai [12] proposed and assessed a model based on a conventional cake filtration theory model. The complexity of their proposed model structure can be very prohibitive for any optimization and control studies.

In the present study, we examined the accuracy and viability of the continuity mass balance equations, reactions kinetics laws, and flux empirical correlations in predicting the dynamic behavior of MBR. The model was validated by collecting experimental data from a prototype apparatus with different numbers of scheduling scenarios and comparing these data with predictions from the developed model. The comparisons include permeate flux, biomass growth rate, and biomass concentration transient behavior. Based on the numerical simulation results, one can optimize a scheduling procedure for MBR without the need to perform experimentation on the actual process.

## 2. Mathematical modeling

Sludge characteristics are directly affected by MBR operating parameters including the sludge retention time (SRT), hydraulic retention time (HRT), food to microorganism ratio (F/M), dissolved oxygen (DO), dilution rate, and organic loading rate (OLR). In contrast, the operating conditions are characterized by the substrate concentration, temperature, aeration, backwashing, and chemical cleaning. Additionally, transmembrane pressure (TMP) is another major factor that affects membrane fouling. TMP is directly related to the permeate flux. High TMP operation increases the transport of foulants to the membrane and increases the permeate flow.

Mathematical model was developed on the aerobic MBR shown in Fig. 1. The system consisted of two inputs and three outputs. The inputs were the influent (i.e. wastewater), and the air from the aerator. The outputs were the effluent or permeate (i.e. treated water with low biomass concentrations), the decayed, floating biomass removed by overflow, and the waste (i.e. accumulated sludge). The representative mathematical model was derived by applying a material balance on three major parameters: substrate concentration ( $S$ ), biomass concentration ( $X$ ), and oxygen concentration ( $O_2$ ) according to the following assumptions: (1) reactor volume was constant due to the overflow; (2) reactor contents were well combined; (3) no biomass in the effluent stream on account of the membrane was impermeable to biomass; (4) no substrate in the overflow, dead biomass stream; and (5) biomass growth rate follows mid-range concentrations kinetics.

Substrate mass balance:

$$V \frac{dS}{dt} = Q_{in} S_{in} - (Q_e S_e + Q_w S_w) + r_{SU} V \quad (1)$$

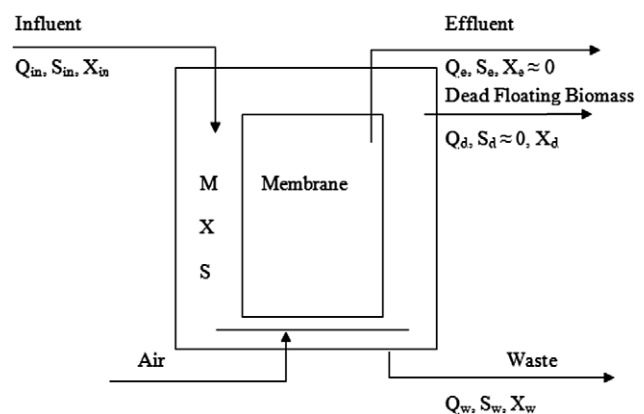


Fig. 1. MBR block flow diagram.

Biomass mass balance:

$$V \frac{dX}{dt} = Q_{in}X_{in} - (Q_wX_w + Q_dX_d) + r_gV \quad (2)$$

Oxygen consumption mass balance:

$$\frac{dO_2}{dt} = D_S(S_{in} - S) - \beta \frac{dX}{dt} \quad (3)$$

where  $\beta$  is the conversion factor of biomass to COD and  $D_S$  ( $\text{time}^{-1}$ ) is the constant dilution rate. The kinetics of the aerobic MBR was described in terms of the rate of substrate utilized for microorganism growth ( $r_{su}$ ), the rate of microorganism growth ( $r_g$ ) consumed or dead ( $r_d$ ), and the rate of oxygen uptake for microorganism respiration ( $r_{O_2}$ ). Furthermore, using Monod-specific biomass growth rate [13], the rate of substrate utilization is

$$r_{SU} = - \left( \frac{\mu_{max}}{Y_{bio}} \right) \frac{SX}{K_S + S} \quad (4)$$

The rate of biomass generated is,

$$r_g = \mu_{max} \left( \frac{SX}{K_S + S} \right) - k_dX \quad (5)$$

and the rate of oxygen uptake is,

$$r_{O_2} = -r_{SU} - 1.42r_g \quad (6)$$

where 1.42 is the COD of cell tissue (mg substrate/mg biomass). Hence, Eqs. (4)–(6) require the estimation of four kinetic parameters using experimental data. These parameters are maximum specific biomass growth rate ( $\mu_{max}$ ), Monod constant ( $K_S$ ), net biomass yield ( $Y_{bio}$ ), and endogenous decay coefficient ( $k_d$ ). An empirical flux model was developed to represent the flux decline as a function of time. Nevertheless, a more representative flux model was required to relate the flux to other design or operating parameters. Darcy's law correlates the flux with both the membrane permeability ( $L_p$ ) in ( $\text{L}/\text{m}^2\text{daykPa}$ ) and pressure gradient ( $\Delta P$ ) or TMP across the membrane in (kPa). SRT is defined as the ratio of biomass accumulated in the MBR to the amount of biomass removed per day. Hence at steady state, from Eq. (2):

$$\text{SRT} = \frac{XV}{Q_wX_w + Q_dX_d} \quad (7)$$

Controlling SRT is essential in order to obtain an acceptable MBR operation. Long SRT reduces the biomass activity while short SRT results in washout

condition. The washout condition is obtained from Eq. (7), when  $Q_wX_w + Q_dX_d$  is greater than  $XV$ . Alternatively, long SRT operation indicates the biomass generation rate is greater than the biomass removal rate. As a result, high sludge viscosities are attained which minimize the oxygen transfer rate (OTR) and thus deactivates the biomass. HRT is defined as the ratio of the volume to the influent volumetric flow rate or the reciprocal of dilution rate. It is also one of the process control parameters that affect membrane fouling. A short HRT or high dilution rates result in high membrane fouling rates due to the production of filamentous bacteria [14]. On the other hand, a long HRT requires a larger MBR volume because of the high influent flow rates. F/M is defined as the ratio of COD or BOD entering the MBR to the Mixed Liquor Suspended Solids (MLSS) concentration in the MBR (mg biomass/mg biomass day) [15]. OLR is defined as the amount of soluble and particulate organic matter fed to the MBR per unit volume ( $\text{kg biomass}/\text{m}^3\text{ day}$ ). High OLR and fluctuation in the OLR lead to unstable process, poor filtration performance, and severe fouling rates. Constant dissolved Oxygen concentration is required to obtain efficient operation in the MBR. Maximizing the OTR between the injected air bubbles and biomass cells is essential to maintain high biomass activity. The following correlation represents the OTR in the MBR.

$$\text{OTR} = Q_{O_2}X = (Y_{O_2/X})r_gX \quad (8)$$

Where:  $Y_{O_2/X}$  is the oxygen transfer yield in ( $\text{g O}_2/\text{g biomass}$ ).

$$Y_{O_2/X} = \frac{r_{O_2}}{r_g} = \frac{\Delta O_2}{\Delta X} \quad (9)$$

Assuming mid-range concentration kinetics

$$\text{OTR} = \left( \frac{\Delta O_2}{\Delta X} \right) \left[ \mu_{max} \left( \frac{SX}{K_S + S} \right) - k_dX \right] X \quad (10)$$

### 3. Experimental work

The MBR experiments were performed at ambient temperature and pressure. The synthetic wastewater was prepared in order to achieve the best microorganism activity inside the MBR. The feed was prepared in a 25-L holding tank T-101 and its composition is shown in Table 1. The experimental setup of the MBR is depicted in Fig. 2. The MBR specifications and the membrane characteristics are shown in Table 2. The

Table 1  
Synthetic wastewater composition

Component	Concentration (g/L)
Acetic acid	31.6
NH <sub>4</sub> Cl	8.8
KH <sub>2</sub> PO <sub>4</sub>	1.3
FeCl <sub>3</sub> ·6H <sub>2</sub> O	0.1
CaCl <sub>2</sub>	0.2
MgSO <sub>4</sub>	0.2
KCl	0.2
NaCl	0.2
NaHCO <sub>3</sub>	49.8

system utilized an air diffuser, a DO measuring probe, control valves, a compressor, and three pumps: piston pump (P-101), vacuum pump (P-102), and backwash

pump (P-103). The synthetic wastewater feed was prepared in tank (T-101), and then pump P-101 was used to pump the feed (stream 1) into the MBR tank (T-102). Tank T-102 consisted of a submerged flat sheet membrane and an air diffuser. The air (stream 5) was compressed through the compressor C-101 and was fed to the MBR through the implemented air diffuser. The treated water (stream 2) was drawn out of the membrane through the vacuum pump P-102. A split stream (stream 3) was taken from the treated water through the backwash pump P-103 and back to the membrane, hence, reversing the direction of water flow through the membrane and cleaning and regenerating the membrane. The remaining treated water (stream 4) was collected in tank T-103. Finally, the accumulated sludge (stream 6) was removed from the bottom of tank T-102.

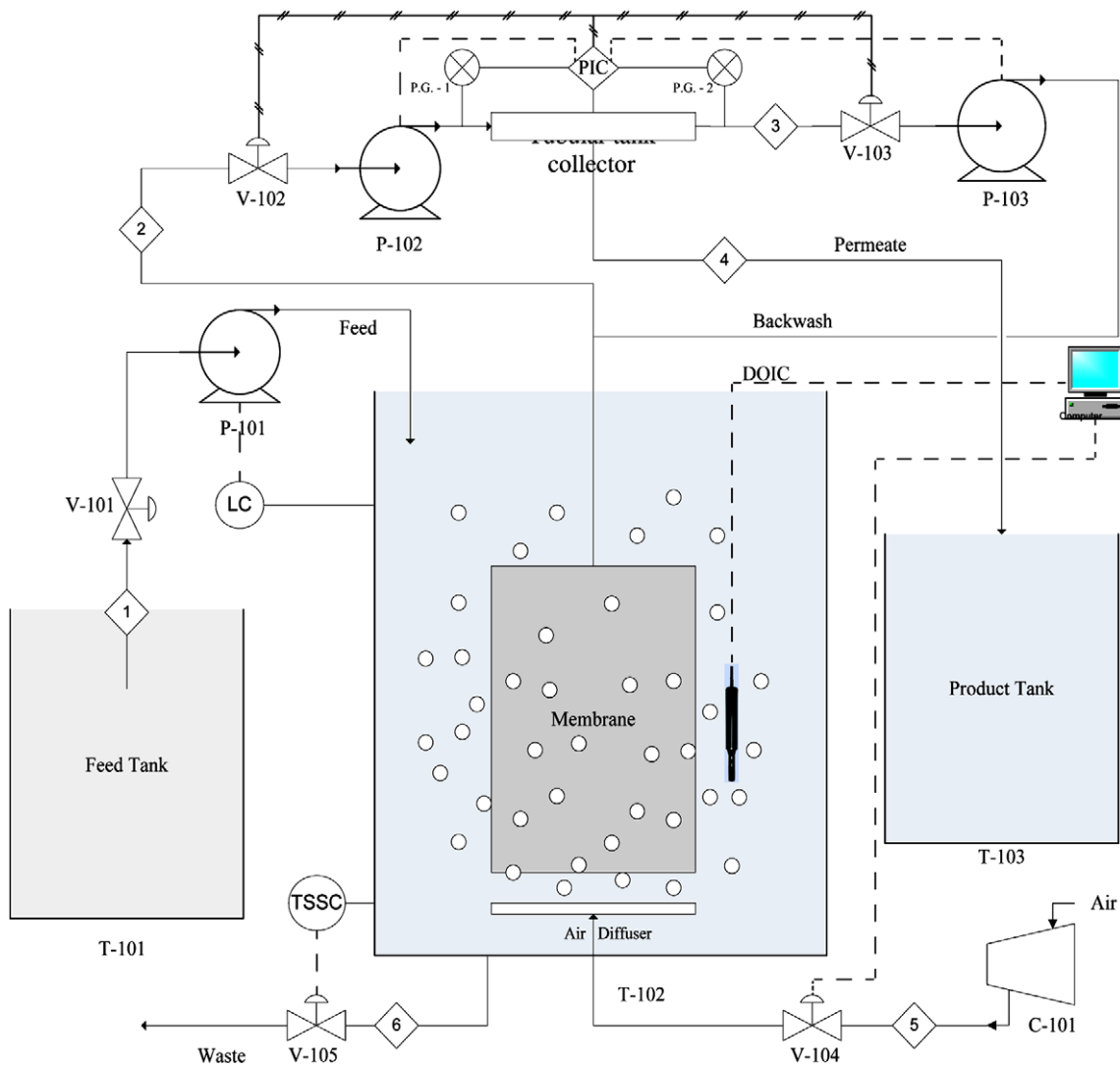


Fig. 2. Membrane bioreactor experimental set-up.

Table 2  
The MBR specifications and the membrane characteristics

MBR	Material of construction	Acrylic
	Dimensions	15 cm × 3 cm × 30 cm
	Effective volume	1 L
	Water depth	30 cm
Membrane	Material of construction	Ceramic
	Model	Flat sheet membrane
	Frame dimensions	12 cm × 12 cm
	Pore size	0.2 μm
	Total surface area	0.048 m <sup>2</sup> (from all sides)

Four control schemes were utilized as shown in Fig. 2. The first was the level controller (LC). An on-off level controller of a float and contactor type was used. As the desired liquid level in the MBR was attained, the LC sent a signal to switch off the feed pump P-101. The second control scheme was the dissolved oxygen control. The DO concentrations were measured through the DO probe utilizing a dissolved oxygen indicator controller (DOIC), which maintained the DO at a setpoint value of 7 mg/l. The DO probe was submerged in the MBR tank T-102 and was continuously monitored through the PC. If the dissolved oxygen concentrations decreased, the PC would send a signal to open valve V-104 in order to increase the aeration rate. The third control scheme was the pressure control across the membrane. Two pressure gages PG1 and PG2 were placed on streams 2 and 3, respectively. The pressure gages were direct indicators of membrane fouling. A decrease in vacuum pressure gage (PG1) implied high filtration pressures and membrane fouling. Therefore, the pressure indicator controller (PIC) sent a signal to switch off pump P-102 and switch on pump P-103 and perform a backwash. As the pressure gage PG2 was stabilized indicating stable operation with no membrane fouling, the PIC controller sent a signal to switch off the backwash pump P-103 and switch on the vacuum pump P-102; hence, filtration was resumed. The fourth control scheme was the total suspended solids controller (TSSC). The TSS concentrations represented the accumulated sludge concentrations. As the TSS level increased, the TSSC transmitted a signal to open valve V-105 that discharged the excess accumulated sludge. The significance of this control scheme represented that an excess of sludge accumulation may block part of the membrane and decreased the membrane selectivity. In addition, a high level of accumulated sludge

might block the air diffuser and thus, effect the overall MBR operation.

Four liters of biomass was prepared by adding two capsules of polyseed (Bioscience Inc.) that contained a mixed culture of microorganisms into distilled water. The mixture was fed with 10 g sugar/day. Then the biomass was incubated for 24 h under aeration by oil-free compressed air through an air diffuser. The preparation of biomass was performed separately before mixing it with the synthetic wastewater feed. The backwash scheduling was performed by applying different vacuum-to-backwash time scenarios and observing the flux decline. The optimum ratio was concluded for the scenario in which the minimum flux decline was observed. Minimum flux decline indicates stable operation and low fouling rates. Another approach was to observe the backwash pressure change. A nearly constant backwash pressure operation indicated low fouling rates.

Experiments were performed utilizing two control schemes. The first scheme was a float and contactor-level controller. The second was a pressure controller scheme utilizing two control valves (Castel Italy) V-102 and V-103. The pressure controller scheme was connected to Siemens LOGO computer software. The software was connected to a contactor to which the power supply of both pumps and control valves were connected. A timer was programmed within the software to specify the vacuum-to-backwash operation scheduling. The software was operated with 10, 20, or 30 min vacuum (or filtration) duration. At the end of each period, the vacuum pump P-102 was switched off and backwash pump P-103 was switched on for 1 or 2 min applying backwash. This procedure was repeated continuously for 90 days duration. After each 15-day interval, a different vacuum-to-backwash time scenario was performed. For the duration, both vacuum and backwash pressures, as the permeate flux, were recorded. Also based on the unit productivity, the permeability was calculated. The turbidity, NH<sub>4</sub>-N<sub>2</sub>, and DO were monitored throughout the experiment duration. The turbidity was measured through turbid meter, NH<sub>4</sub>-N<sub>2</sub> was analyzed by Direct Nesslerization, and DO concentrations were measured through a DO probe. Furthermore, the results of the biomass concentration decay during filtration period were recorded and further used in biomass mass balance solution methods.

#### 4. Results and discussion

Inevitably membrane filtration performance decreases with filtration time due to fouling. The permeate flux decline is a direct indication of membrane

fouling phenomena. It is determined by several factors, such as substrate composition, membrane properties (geometry, configuration, pore size, and material of construction), and operation conditions (HRT, aeration rate, TMP, etc.). Moreover, the permeate flux behavior is observed as a sharp flux decline at the beginning, followed by a gradual decline due to reversible fouling and concentration polarization, and finally steady-state operation is obtained due to irreversible fouling. This behavior was also demonstrated in our previous work, Aidan et al. [9]. Fig. 3 shows an exponential decline of the flux during the MBR operation at different backwash scheduling. The flux started to decline from an initial or pure water flux across the membrane (7.3 L/m<sup>2</sup>h) where there was no accumulation of foulants on the membrane. The flux behavior was obtained under different backwash scheduling scenarios. The different vacuum time (vac) durations were 10, 20, and 30 min, while the backwash durations (bw) were 1 and 2 min. Each vacuum time was tested with both backwash durations.

Mallubhotla et al. [11] suggested a flux empirical model that might describe such phenomena. By defining the initial water flux as  $J_0$ , the following model was suggested.

$$J(t) = J_0 \cdot e^{\frac{-t}{A+Bt}} \tag{11}$$

The function  $f(t)$  in Eq. (11) defines the time constants of the flux. The sharper the flux decline, the higher the order of the function  $f(t)$ . Assuming the function to be a linear first order, the following flux empirical model was obtained.

$$J(t) = J_0 \cdot e^{\frac{-t}{A+Bt}} \tag{12}$$

where  $A$  is time constant for cake growth in (days) and  $B$  is the cake growth constant. The flux model in Eq. (11) agrees with the observed flux behavior in terms of the exponential decline and the steady-state behavior. The steady-state behavior may be obtained from Eq. (12) at long operation period as follows:

$$Ast \rightarrow \infty J(\infty) \rightarrow J_0 \cdot e^{\frac{-1}{B}} \tag{13}$$

The flux from Eq. (13) reflects a constant value indicating the steady-state flux. It consists of two constant terms the initial flux ( $J_0$ ) and the exponential term with respect to the cake growth constant ( $B$ ). Nevertheless, the derived flux empirical model in Eq. (12) explains the flux behavior with respect to operation time. Hence, a more representative flux model is required to express the flux in terms of other operation parameters such as TMP and vacuum-to-backwash time ratio.

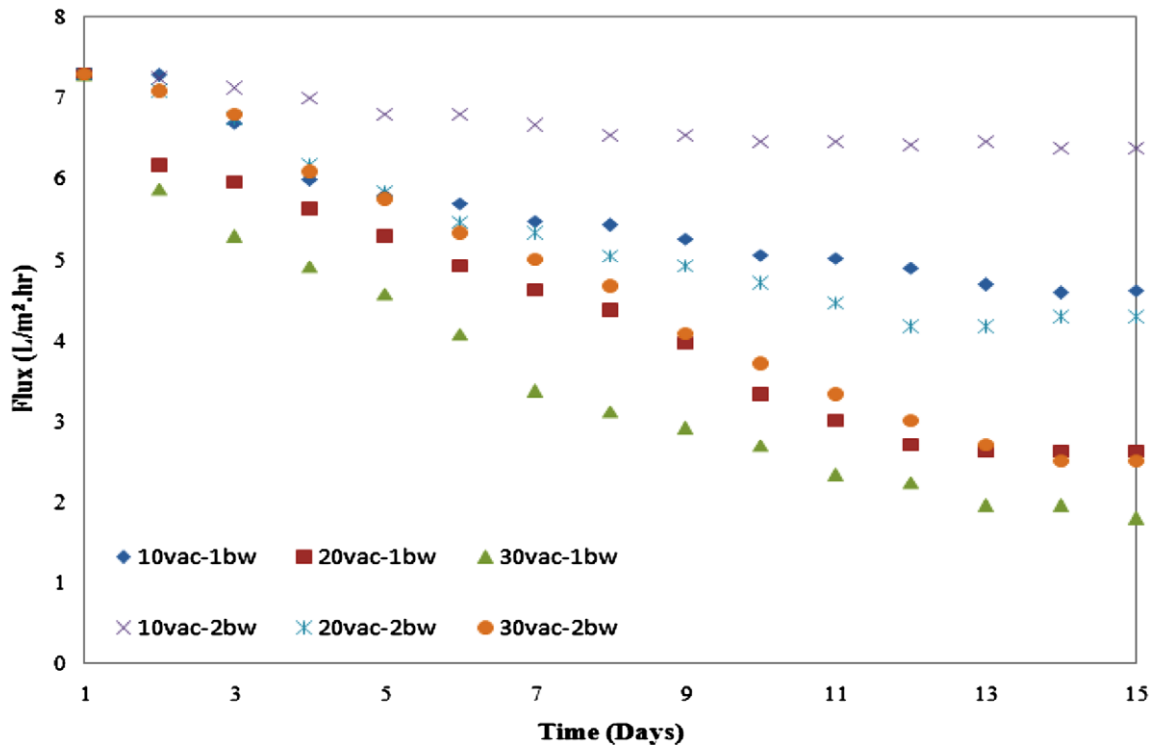


Fig. 3. Flux decline curve for various vacuum-to-backwash times.

Table 3  
Kinetic parameters estimation

$\mu_{\max}$ (g new biomass/ g biomass day)	185
$Y_{\text{bio}}$ (g biomass/ g phenol)	0.0195
$K_s$ (g phenol/m <sup>3</sup> )	$1.01 \times 10^5$
$k_d$ (g dead cells/g cells day)	0.165

More experiments were performed using the optimum backwash-to-vacuum time ratio obtained from this work and previous works, i.e. 10 min vacuum to 2 min backwash (Aidan et al. [9]). The COD concentrations in both influent and effluent were used in kinetic parameters estimation. The developed kinetic model requires the estimation of four kinetic parameters, namely: the maximum specific biomass growth rate ( $\mu_{\max}$ ), the Monod constant ( $K_s$ ), the net biomass yield ( $Y_{\text{bio}}$ ), and the endogenous decay coefficient ( $k_d$ ). The kinetic model parameters were estimated by reconciling the model output with data obtained from the experimental work. The kinetic parameters were calculated using nonlinear regression. The estimated kinetic model parameters are summarized in Table 3 and kinetic model was compared to the data as shown in Fig. 4.

Fig. 4 is a plot of kinetic model calculation of microorganism growth ( $r_{\text{su}}$ ) vs. experimental data

with a regression of 0.83. There is reasonable agreement between the experimental data and the model estimation which may indicate that the assumption of middle-range concentration kinetics for biomass growth is valid. Moreover, Fig. 4 shows the decline of substrate utilization rate with time. This is attributed to the high substrate consumption rates in biomass growth. After estimating the kinetic parameters, the biomass dynamic model was solved and validated to experimental data. The biomass dynamic model in Eq. (2) was solved with the following assumptions: (1)  $X_d \ll X_w$ ; (2)  $X_{\text{in}} \cong 0$  (no biomass in the feed); and (3)  $K_s \gg S$  (see Table 3). Solving the dynamic biomass model yielded the following equation.

$$X = X_o \left[ \exp \left( - \left( \frac{\mu_{\max}}{K_s} \right) S - D_w + k_d \right) t \right] \quad (14)$$

$D_w$  in Eq. (14) represents the waste dilution rate. It is defined as the ratio of the waste volumetric flow rate to the MBR volume ( $D_w = Q_w/V$ ). The waste dilution rate was estimated using the obtained experimental data. Nonlinear regression was utilized for the dilution rates estimation. The influent dilution rate ( $D_{\text{in}}$ ) was found to be  $361 \text{ day}^{-1}$  and the effluent dilution rate ( $D_w$ ) was  $65 \text{ day}^{-1}$ . The results indicated a higher influent flow compared to effluent flow. The lower effluent dilution rate may be attributed to membrane

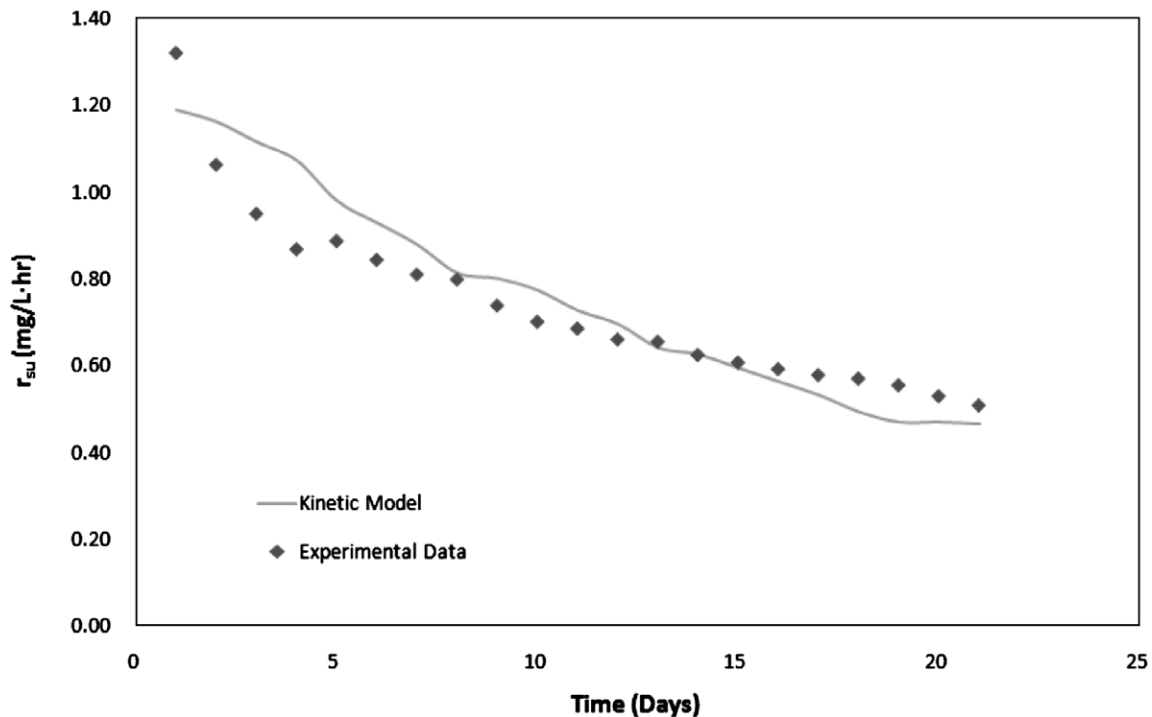


Fig. 4. Kinetic model prediction of microorganism growth ( $r_{\text{su}}$ ) vs. experimental data.

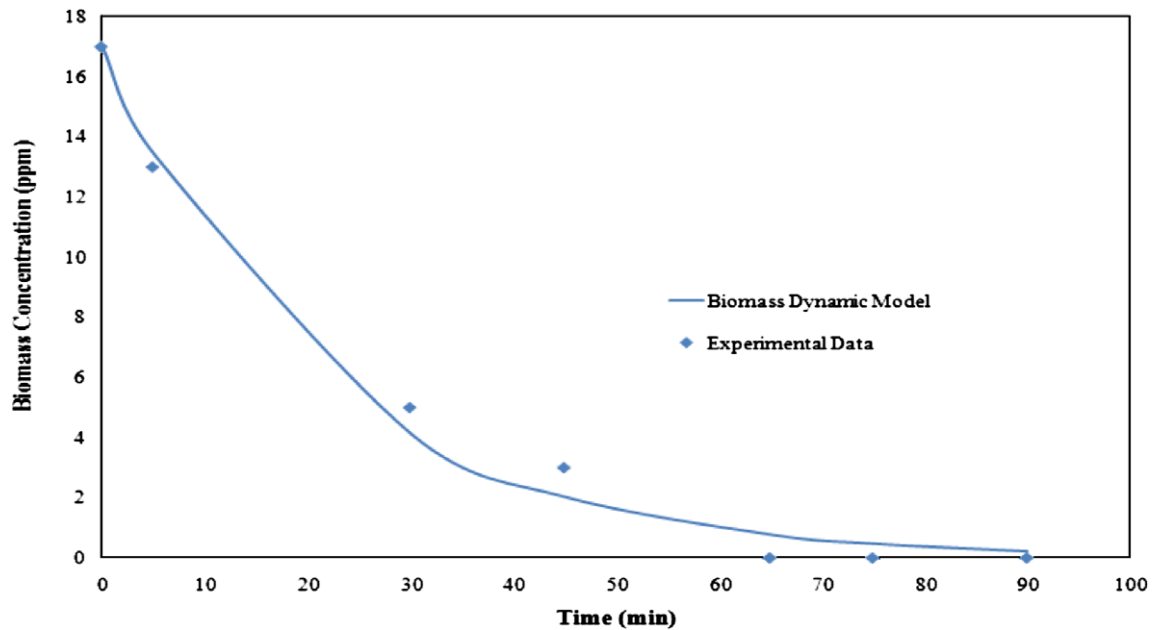


Fig. 5. Model prediction of biomass concentration dynamics vs. experimental data.

fouling or pore blocking. Furthermore, the transient biomass concentration was calculated from Eq. (14) using both the estimated waste dilution rate and the estimated kinetic parameters. It was further plotted with the corresponding experimental data as in Fig. 5. A reasonable agreement was obtained with a coefficient of determination of 0.932.

Fig. 5 shows the transient biomass concentration declines with time. The transient decline of biomass concentration indicates high biomass removal rates. As more foulants were retained by the highly selective membrane, the accumulated fouling layer thickness increased. The growing fouling layer enhances the filtration performance as it acts as a pre-filter. Furthermore, Fig. 5 demonstrates a decent affiliation of the biomass model to experimental data. This verifies both the estimated kinetic parameters and the developed biomass process model. The flux empirical model in Eq. (12) requires the estimation of two parameters  $A$  and  $B$  using experimental data. The obtained experimental data give the flux decline as a function of time for different backwash-to-vacuum time scheduling scenarios. The two parameters were

estimated for each run using nonlinear regression. Flux parameters estimation results are summarized in Table 4 and are plotted in Fig. 6 with an average regression of 0.96.

As illustrated in Fig. 6, the flux empirical model shows a reasonable conjunction to experimental data at different backwash scheduling scenarios (15 days interval). Nevertheless, the estimated flux parameters in Table 4 varied significantly at different operating conditions (i.e. different backwash scheduling). Thus, any changes in the MBR operating conditions (i.e. due to disturbance) will require re-calculation of both parameters ( $A$  and  $B$ ). Consequently, the indicated empirical model was neither accurate nor representative to the flux dynamics in the MBR. Hence, a more representative dynamic flux model is needed. The flux model should relate the flux to different operation variables such as vacuum pressure, backwash pressure, and backwash scheduling. Darcy's law describes the flux as a function of pressure gradients. However, observing the flux behavior in Fig. 6 indicates the large effect of backwash scheduling on the flux decline.

Table 4  
Flux empirical model parameters estimation

Ratio (vacuum minutes to backwash minutes)	10 to 1	20 to 1	30 to 1	10 to 2	20 to 2	30 to 2
$A$ (days)	23.2	16.1	10.1	69.0	22.1	23.7
$B$ (days)	0.517	-0.221	0.005	2.28	0.173	-0.769

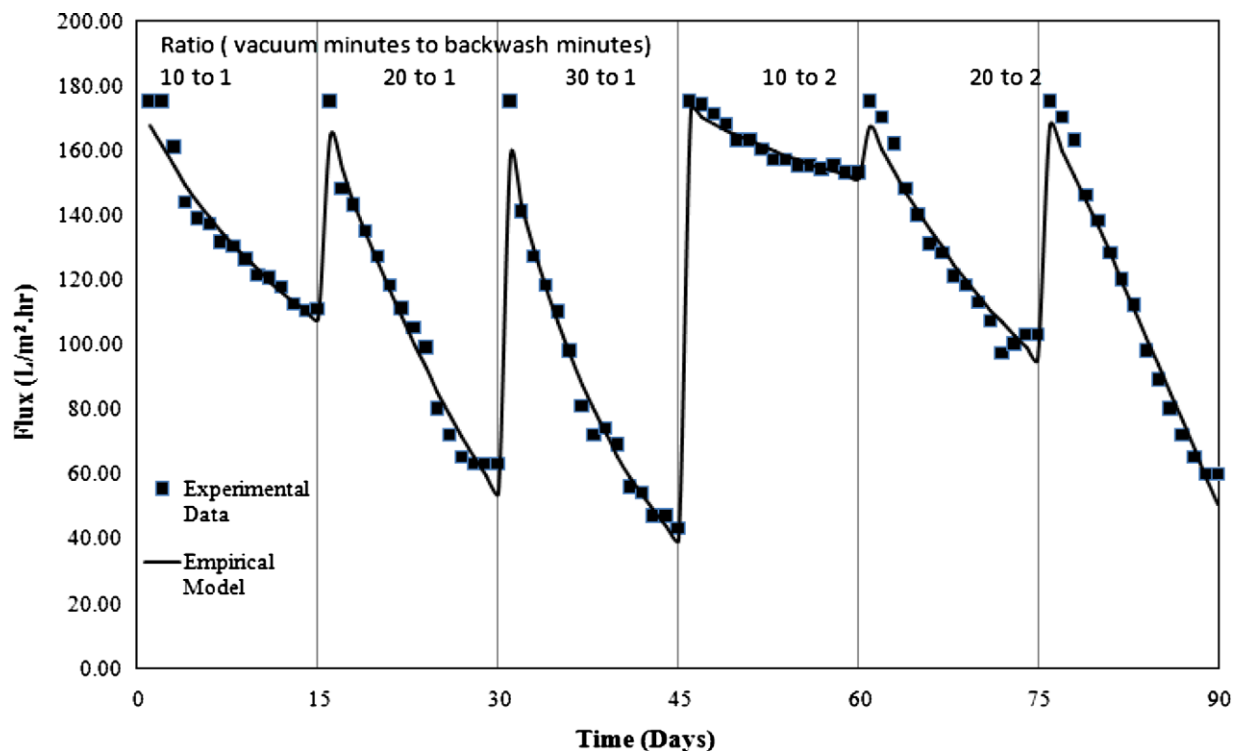


Fig. 6. Model prediction vs. experimental data of flux dynamics.

## 5. Conclusions

The proposed dynamic model captured the dynamic behavior of the MBR. The flux empirical model had reliable estimates of the flux at different backwash scheduling scenarios. However, the flux empirical model parameters estimation was found to be sensitive to different operating conditions. The generated numerical simulation results will be employed in future work to develop a black-box model such as artificial neural networks (ANNs) that will correlate flux to backwash and vacuum times in order to optimize and control membrane fouling.

## References

- [1] F. Meng, S.R. Chae, A. Drews, M. Kraume, H.S. Shin, F. Yang, Recent advances in membrane bioreactors (MBRs): Membrane fouling and membrane material, *Water Res.* 43 (2009) 1489–1512.
- [2] H. Chio, K. Zhang, D.D. Dionysios, D.B. Oerther, G.A. Sorial, Effect of permeate flux and tangential flow on membrane fouling for wastewater treatment, *Sep. Purif. Technol.* 45 (2005) 68–78.
- [3] S.P. Hong, T.H. Bae, T.M. Tak, S. Hong, A. Randall, Fouling control in activated sludge submerged hollow fiber membrane bioreactor, *Desalination* 143 (2002) 219–228.
- [4] M. Gander, B. Jefferson, S. Judd, Aerobic MBRs for domestic wastewater treatment: A review with cost considerations, *Sep. Purif. Technol.* 18 (2000) 119–130.
- [5] N.O. Yigit, G. Civelekoglu, I. Harman, H. Koseoglu, M. Kitis, Effects of various backwash scenarios on membrane fouling in a membrane bioreactor, *Desalination* 237 (2009) 346–356.
- [6] J. Wu, P. Le-Clech, R.M. Stuetz, A.G. Fane, V. Chen, Effects of relaxation and backwashing conditions on fouling in membrane bioreactor, *J. Membr. Sci.* 324 (2008) 26–32.
- [7] K. Matsumoto, M. Katsuyama, H. Ohya, Separation of yeast by cross-flow filtration with back-washing, *J. Ferment. Technol.* 65(1) (1987) 77–83.
- [8] T. Jiang, M.D. Kennedy, B.F. Guinzbourg, P.A. Vanrolleghem, J.C. Schippers, Optimizing the operation of a MBR pilot plant by quantitative analysis of the membrane fouling mechanism, *Water Sci.* 51(6–7) (2005) 19–25.
- [9] A. Aidan, N. Abdel-Jabbar, T.H. Ibrahim, V. Nenov, F. Mjalli, Neural network modeling and optimization of scheduling backwash for membrane bioreactor, *Clean Technol. Environ. Policy* 10(4) (2007) 389–395.
- [10] S.G. Redkar, R.H. Davis, Crossflow microfiltration with high frequency reverse filtration, *AIChE J.* 41 (1995) 501–508.
- [11] H. Mallubhotla, G. Belfort, Semiempirical modeling of cross-flow microfiltration with periodic reverse filtration, *Ind. Eng. Chem. Res.* 35 (1996) 2920–2928.
- [12] C. Tien, R. Bai, An assessment of the conventional cake filtration theory, *Chem. Eng. Sci.* 58 (2003) 1323–1336.
- [13] Y. Xu, J. Dodds, D. Leclerc, Optimization of a discontinuous microfiltration-backwash process, *Chem. Eng. J.* 57 (1995) 247–251.
- [14] H. Scott Fogler, *Elements of Chemical Reaction Engineering*, fourth ed., Prentice Hall, Upper Saddle River, NJ, 2006.
- [15] F. Meng, B. Shi, F. Yang, H. Zhang, Effect of hydraulic retention time on membrane fouling and biomass characteristics in submerged membrane bioreactors, *Bioprocess Biosyst. Eng.* 30 (2007) 359–367.